

Activation of extracellular signaling regulated kinase in natural killer cells and monocytes following IL-2 stimulation in vitro and in patients undergoing IL-2 immunotherapy: analysis via dual parameter flow-cytometric assay

Sri Vidya Kondadasula · Kimberly A. Varker · Gregory B. Lesinski · Don M. Benson Jr · Amy Lehman · Thomas Olencki · J. Paul Monk · Kari Kendra · William E. Carson III

Received: 20 February 2007 / Accepted: 17 December 2007 / Published online: 10 January 2008
© Springer-Verlag 2008

Abstract Interleukin-2 (IL-2) activates extracellular signal-regulated protein kinase (ERK) within immune cells. To examine the profile of phosphorylated ERK (p-ERK) in IL-2 stimulated immune cells of normal donors and patients receiving IL-2 therapy, we developed a dual parameter flow-cytometric assay. An analysis of PBMCs stimulated with IL-2 indicated that IL-2 exposure induced p-ERK in CD56^{bright} NK cells and CD14⁺ monocytes, but not in CD3⁺ T cells or CD21⁺ B cells. CD3⁺ T cells that were induced to express functional high-affinity IL-2R did not exhibit enhanced p-ERK following IL-2 treatment. Measurement of p-ERK within PBMCs from cancer patients 1 h following their first dose of IL-2 revealed a complete absence of circulating NK cells, consistent with earlier observations. However, the total number of circulating CD14⁺ monocytes increased in these samples and 97% of these cells exhibited

ERK activation. p-ERK was not observed in T cells post-IL-2 therapy. Analysis of PBMCs obtained 3 weeks post-IL-2 therapy revealed high-p-ERK levels in CD56^{bright} NK cells in a subset of patients, while levels of p-ERK returned to baseline in monocytes. These studies reveal an effective method to detect ERK activation in immune cells and demonstrate that IL-2 activates ERK in a subset of NK cells and monocytes but not T cells.

Keywords Flow-cytometry · Interleukin-2 · ERK · Natural killer cell · T Cells · Monocyte

Introduction

Interleukin-2 (IL-2) is an immunoregulatory cytokine that is produced primarily by activated CD4⁺ T cells to support their growth and clonal expansion [15]. IL-2 interacts with the heterodimeric (IL-2R $\beta\gamma$) or heterotrimeric (IL-2 $\alpha\beta\gamma$) IL-2 receptor (IL-2R) on the target cell surface to mediate its effects. IL-2 activates multiple signaling pathways in immune effectors upon binding to its receptor, including the Ras-mitogen activated protein kinase (Ras/MAPK pathway), the Janus-kinase (JAK)-signal transducer and activator of transcription (STAT) pathway, and the phosphoinositide 3-kinase (PI 3-kinase) pathway [6, 11, 20]. Although the precise functional role of each of these signaling pathways is still under investigation, IL-2 induced activation of the Ras/MAPK pathway is known to promote cell survival and proliferation. IL-2 stimulates this signaling pathway via the recruitment of the adaptor protein Shc [Src homology 2 domain (SH2) containing protein] to the acidic domains of the IL-2R β subunit. This further results in formation of a Shc-Grb2-SOS trimolecular complex that triggers the downstream Ras/MAPK cascade, with eventual

S. V. Kondadasula · G. B. Lesinski · W. E. Carson III
Human Cancer Genetics Program,
Department of Molecular Virology,
Immunology and Medical Genetics,
The Ohio State University, Columbus, OH 43210, USA

K. A. Varker · W. E. Carson III (✉)
Department of Surgery, The Ohio State University,
N924 Doan Hall, 410 West 10th Avenue,
Columbus, OH 43210, USA
e-mail: william.carson@osumc.edu

D. M. Benson Jr · T. Olencki · J. P. Monk · K. Kendra
Department of Internal Medicine, The Ohio State University,
Columbus, OH 43210, USA

A. Lehman
Center for Biostatistics, The Arthur G. James Comprehensive
Cancer Center, Solove Research Institute,
The Ohio State University, Columbus, OH 43210, USA

activation of extracellular signaling regulated kinase (ERK) [9]. ERK consists of two closely related isoforms; ERK1 and ERK2 that are 42 and 44 kDa in size, respectively. Activation of ERK induces its nuclear translocation, whereupon it regulates the expression of transcription factors such as AP-1 and Elk-1 [8, 22]. These factors subsequently induce the transcription of several genes that are involved in the cell cycle progression and the prevention of apoptosis [2].

Clinically, IL-2 is used to treat patients with metastatic malignant melanoma or renal cell carcinoma. It induces complete or partial responses in 10–20% of patients, and about one-third of these individuals will experience a durable complete response [1]. However, toxicity involving multiple organ systems can occur following the administration of high-dose IL-2, and therefore patients must be carefully selected [12, 13]. Previous studies have suggested that the clinical response to IL-2 immunotherapy is mediated through *in vivo* expansion and activation of cytotoxic lymphocytes and/or enhanced migration of cytotoxic lymphocytes within host tissues [23], although the precise signaling pathways responsible for mediating these effects are not known.

A comprehensive analysis of ERK-mediated signal transduction in immune cell subsets following IL-2 activation has not been performed thus far, due in part to the constraints of current analytic techniques. We developed a dual parametric flow-cytometry assay that permits the evaluation of ERK activation in immune cell subsets following IL-2 stimulation. We hypothesized that flow-cytometric analysis of ERK-mediated signaling events within immune cell subsets could provide further insight into the mechanism of action of IL-2 in cancer patients [10]. In the present report, we demonstrate that ERK was activated within CD56^{bright} NK cells, which is a subset of CD56⁺ NK cells [5] and CD14⁺ monocytes, but not in CD4⁺ or CD8⁺ T cells following IL-2 treatment. These results were confirmed *in vivo* following administration of IL-2 to patients with advanced malignancy.

Materials and methods

Reagents

Recombinant human IL-2 with specific activity of 1×10^6 IU/mL (6.6 μ M) was obtained from Hoffmann-La Roche Pharmaceuticals (Nutley, NJ, USA). The stock solution was reconstituted with 33.3 mL of 0.9% saline to obtain a working concentration of 200 nM for the *in vitro* studies. All patients in the study received recombinant human IL-2 (Proleukin[®]; specific activity = 18×10^6 IU/mg) provided by Chiron Corporation (Emeryville, CA,

USA). Phorbol myristate acetate (PMA) was obtained from Sigma Aldrich (St. Louis, MO, USA). Rabbit polyclonal anti-pERK1/2 (Thr²⁰²/Tyr²⁰⁴) was purchased from Cell Signaling Technology (Beverly, MA, USA). Goat polyclonal anti-ERK was purchased from Santa Cruz Biotechnology (Santa Cruz, CA, USA). Rabbit polyclonal anti-p-STAT5 antibody was purchased from Cell Signaling Technology (Beverly, MA, USA). NKH-1 RD1 mouse anti-human CD56 monoclonal antibody (mAb) and APC-conjugated mouse anti-human CD14 mAb were obtained from Immunotech/Beckman Coulter (Fullerton, CA, USA). APC-conjugated mouse anti-human CD3 mAb was obtained from BD Biosciences (San Diego, CA, USA). FITC-conjugated goat anti-rabbit IgG was purchased from Santa Cruz Biotechnology (Santa Cruz, CA, USA). Normal mouse and goat IgG were purchased from Sigma Aldrich (St. Louis, MO, USA). PE-conjugated anti-CD25, CD122, and CD132 monoclonal antibodies from BD Biosciences (San Diego, CA, USA) were a kind gift from Dr. Michael A. Caligiuri, Columbus, OH, USA. RosetteSep NK cell and T cell antibody cocktails were purchased from StemCell Technologies, Vancouver, BC, Canada. Ficoll-Paque (Amersham Pharmacia Biotech Uppsala, Sweden) was used for density gradient separation of PBMCs.

Procurement of peripheral blood mononuclear cells

Normal peripheral blood mononuclear cells (PBMCs) were obtained from healthy adult blood donors (source leukocytes, American Red Cross, Columbus, OH, USA), or from patients with metastatic melanoma or metastatic renal cell carcinoma ($n = 8$ patients) receiving treatment at the Ohio State University Comprehensive Cancer Center under an Institutional Review Board-approved protocol (OSU 99H0348 and OSU 0390, respectively). Patient blood samples were drawn prior to, and 1 h following treatment with the first dose of IL-2 (Proleukin[®]). One cycle of therapy consisted of 600,000 IU/kg (0.037 mg/kg) of IL-2 administered intravenously every 8 h for up to 12 doses. Cycles were repeated at 3-week intervals in the event of a clinical response or stable disease. One patient in this study was treated on a Phase II trial of high-dose IL-2 (720,000 IU/kg, *i.v.*) in combination with a peptide vaccine containing gp 100:209–217 (210M) (OSU IRB #2003C0046) (Table 1). We also obtained blood samples 3 weeks after the first cycle of IL-2 treatment from three patients. PBMCs were isolated from patient peripheral blood by Ficoll-Paque density gradient centrifugation.

Intracellular staining for p-ERK

Cells (2×10^5 per condition) were resuspended in 100 μ L of RPMI-1640 medium, treated with PBS or IL-2,

Table 1 Clinical correlative information for patients receiving the first cycle of IL-2 immunotherapy

Patient	Diagnosis	Site of metastasis	IL-2 dose (IU/kg every 8 h)	Number of cycles received	Number of cells pre-IL-2/post-IL-2	CD14 ⁺ cells expressing p-ERK 1 h post-IL-2 treatment (%) ^b	Clinical response	Toxicity	Status
A	Renal cell carcinoma	Bone (pelvis)	600,000	4	17.96/30.18	89.26	Minor response	Expected ^c	Off treatment
B	Renal cell carcinoma	Bone (vertebral and sacral), hepatic	600,000	1	19.43/61.52	91.11	Unknown	Expected ^c	Off treatment
C ^d	Renal cell carcinoma	Hepatic, single pulmonary nodule	600,000	4	8.37/20.8	92.71	Mixed response ^e	Expected ^c	Off treatment
D	Renal cell carcinoma	Pulmonary	600,000	3	6.44/30.94	97.8	Partial response	Non-oliguric renal insufficiency	Off treatment
E	Ocular melanoma	Hepatic	600,000	4	3.68/16.88	79.33	Mixed response ^e	Expected ^c	Off treatment due to progressive hepatic metastases
F	Melanoma	Subcutaneous, hepatic, adrenal, axillary adenopathy, bilateral breast, frontal lobe (s/p γ knife)	600,000	2	15.49/40.6	70.18	Progressive disease	Expected ^c	Receiving systemic chemotherapy
G ^{a, d}	Melanoma	Local recurrence, solitary pulmonary nodule	720,000	4	3.03/38.85	97.1	Progressive disease	Expected ^c	Off treatment
H ^d	Melanoma	Bilateral pulmonary, subcarinal mass, cerebellar tumor (s/p resection)	600,000	2	7.91/32.35	21.73	Minor response	Staph. infection after IL-2	On therapy

^a On a trial of high-dose IL-2 (700,000 IU/kg every 8 h) with or without peptide vaccine

^b Percent cells expressing p-ERK 1 h post-IL-2 treatment

^c Expected toxicities may include: hypotension, renal insufficiency, tachycardia, rigors, fluid shifts/capillary leak, anemia, lymphopenia, hypocalcemia, hypophosphatemia, hypokalemia, and hypomagnesemia

^d Blood available at 3 weeks post-IL-2 therapy

^e >25% reduction in the size of some lesions and increase in the size in the other lesions

fixed with Fix and Perm Reagent A (Caltag Laboratories, Burlingame, CA, USA) for 2–3 min at room temperature, and then incubated at 4°C for 10 min in 3 mL of cold methanol. Cells were then washed in flow buffer (PBS supplemented with 5% FBS) and permeabilized with 100 μ L of Fix and Perm Reagent B (Caltag Laboratories). Cells were incubated for 30 min at room temperature in Fix and Perm Reagent B containing 0.1 μ g of a rabbit anti-human p-ERK antibody, or an appropriate isotype control antibody. Non-specific binding was blocked with goat IgG and/or mouse IgG, as appropriate. Cells were then washed with flow buffer and incubated with a fluorescein isothiocyanate (FITC)-conjugated goat anti-rabbit secondary antibody for 30 min at room temperature. For subset analysis, cells were also incubated with appropriate extracellular antibodies as a final step in the staining protocol. Cells were then washed with flow buffer, fixed in 1% formalin, and stored at 4°C until flow-cytometric analysis.

Flow-cytometric analysis

Analyses were performed as previously described using a Becton Dickinson FACSCalibur flow-cytometer (Becton-Dickinson, San Jose, CA, USA) [10]. PBMCs were gated in the region of the lymphocyte population as determined by forward light-scatter and side light-scatter properties for the analysis of CD3⁺ T cells, CD56⁺ NK cells, and CD21⁺ B cells. However, for the analysis of monocytes, PBMCs were gated in both lymphocyte and monocyte regions. Subsequently, voltage measurements were obtained for samples stained with isotype control Abs. The voltage was adjusted so that all cells stained with isotype control Abs fell within the first log of fluorescence. Data was obtained by collecting at least 10,000 events for each determination. The detection of p-ERK in NK cells was performed by analyzing fluorescence of the fluorescein conjugate (FITC) in the FL1 channel (488 nm) and NK-RD1 in the FL2 channel following excitation with a 633 nm helium–neon laser. Similarly, activation of ERK in cells stained with allophycocyanin (APC) conjugated CD3, CD14, and CD21 Abs was measured in the FL4 channel utilizing 633 nm helium–neon lasers. Results from dual parametric analysis were displayed on four-decade log scales, where each dot represents a single cell of varying fluorescence in two channels. Quadrants were selected for each fluorochrome based on the above criteria and positive cells were those that displayed fluorescence greater than the background staining obtained with appropriate isotype control Abs. Data files were analyzed using the WinMDI software (created by Joseph Trotter; available at: <http://flowcyt.salk.edu/software.html>).

Immunoprecipitation and western blotting

PBMCs (5×10^6 cells) isolated from source leukocytes obtained from healthy adult donors were cultured for 15 min in RPMI-1640 and either PBS or IL-2. Cell lysates were prepared in general lysis buffer (500 mM Tris, pH 6.8, 0.5 mM EDTA, 1 mM Na₄P₂O₇, 10 mM NaF, 10% SDS, 1 mM Na₃VO₄, and 10 μ g/ml each aprotinin and leupeptin), and post-nuclear lysates were boiled in an equal volume of 2 \times SDS sample buffer [125 mM Tris–HCl (pH 6.8), 4% SDS, 10% glycerol, 0.01% bromphenol blue, and 2% 2-mercaptoethanol] for 5 min. Proteins were separated by SDS-PAGE, transferred to nitrocellulose filters, probed with the p-ERK primary antibody and developed by enhanced chemiluminescence. A β -actin antibody or total ERK antibodies were used to confirm equal loading (Sigma, St. Louis, MO, USA).

Statistics

Basic summary statistics were performed for each of the endpoints. Analysis of variance (ANOVA) was used to assess p-ERK levels for different IL-2 dose levels, as well as to compare p-ERK levels in different immune cell subsets. Random effect models were applied to the data in order to assess trends in p-ERK over time for both PBS and IL-2 treated cells. An $\alpha = 0.05$ level of significance was used for all comparisons. All analyses were performed using SAS version 9.1 (SAS Institute Inc., Cary, NC, USA).

Results

Flow-cytometric analysis of p-ERK in PMA-stimulated cells

The utility of a flow-cytometric assay for the detection of phosphorylated ERK (p-ERK) in immune cells was evaluated in PBMCs isolated from healthy adult donors and in the Jurkat T cell line. Cells that have been treated with PMA (50 ng/ml) for 10 min exhibited a rapid increase in p-ERK as compared to PBS-treated cells. These results were confirmed for an aliquot of cells from each condition via immunoblot analysis of whole-cell lysates utilizing the identical anti-p-ERK antibody (Fig. 1). The flow-cytometric assay detected p-ERK in more than 97% of PMA treated cells and was able to detect baseline phosphorylation of ERK in untreated cells. Flow-cytometry required only 2×10^5 cells per condition, but meaningful data could be obtained in 3 h using as few as 1×10^5 cells (data not shown). Thus, in addition to being rapid, reproducible, and

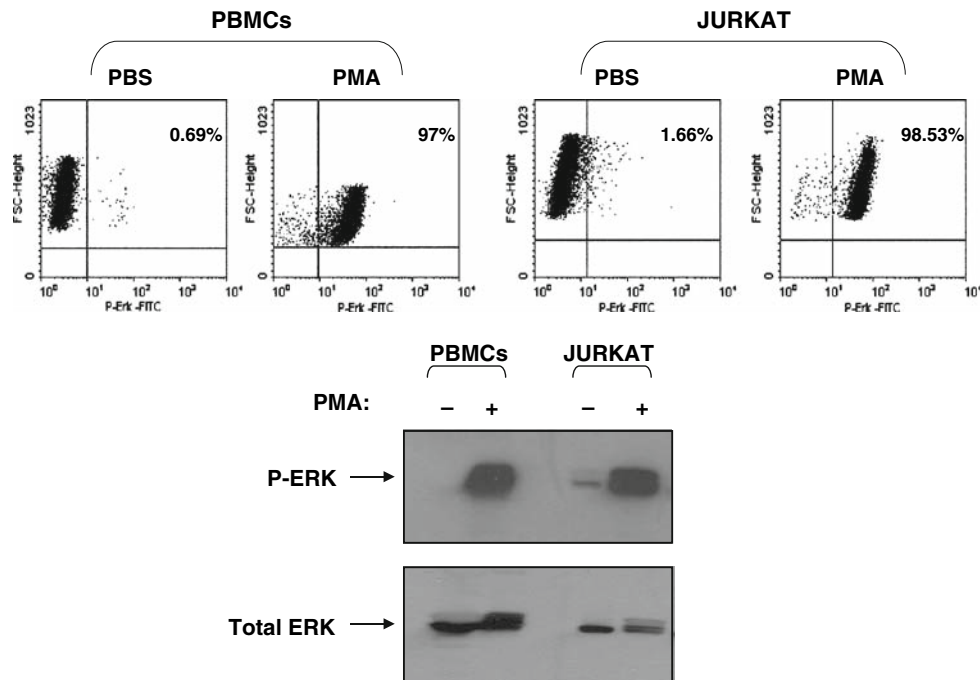


Fig. 1 Flow-cytometric analysis of phosphorylated extracellular signaling regulated kinase (p-ERK) in PMA-stimulated cells and validation by immunoblot analysis. Freshly isolated peripheral blood mononuclear cells (PBMCs) ($n = 4$ donors) and Jurkat T cells were stimulated with phosphate-buffered saline (PBS) or 50 ng/mL of phorbol myristate acetate (PMA) for 10 min at 37°C and analyzed for p-ERK by intracellular flow-cytometry as described in “Materials and methods”. The *x*-axis of the histogram represents p-ERK, while the *y*-axis represents the forward scatter (FSC) of the lymphocyte gated

cells (*upper panel*). Quadrants were set using appropriate isotype control antibodies. The percentage of cells positive for p-ERK is given in the *upper right hand corner*. The flow-cytometric results were confirmed by immunoblot analysis using the same anti-p-ERK antibody (*lower panels*). Whole-cell lysates were prepared from aliquots of cells (5×10^6) that were processed simultaneously for flow-cytometric and immunoblot analysis. Total ERK levels were measured as loading control. Representative data from a single experiment is shown

quantitative, this method required tenfold fewer cells per condition than immunoblot analysis.

Flow-cytometric analysis of p-ERK in IL-2-stimulated cells

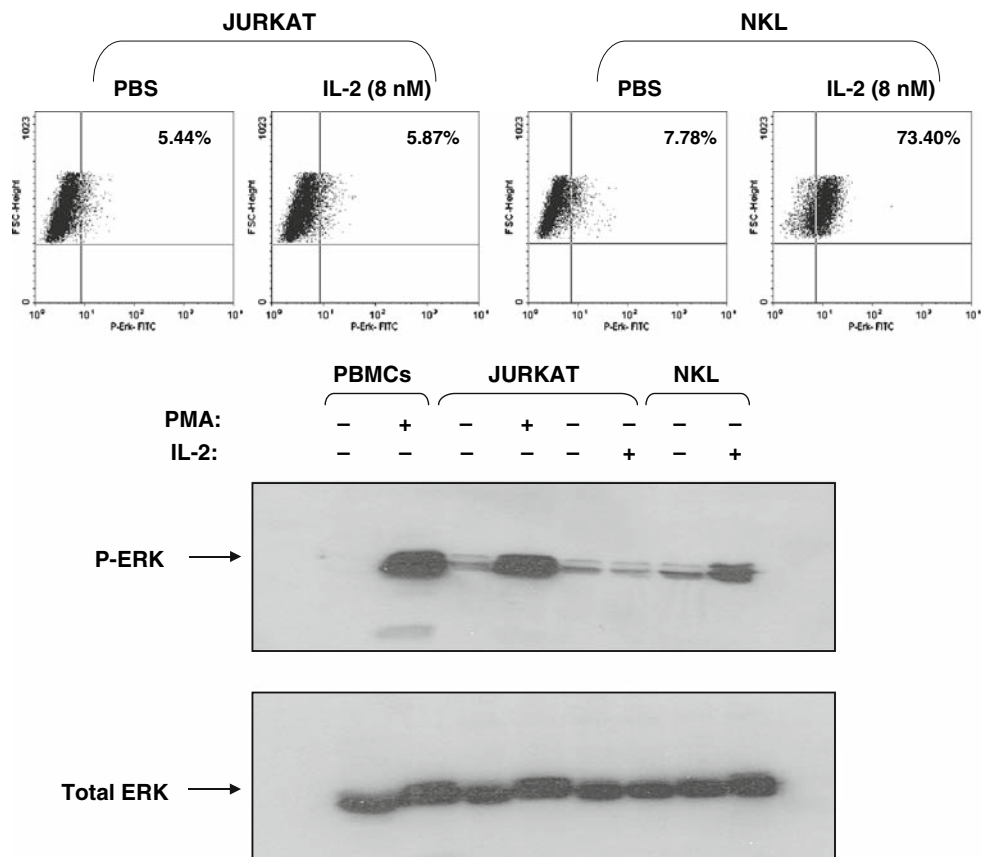
Activation of ERK in response to IL-2 stimulation (8 nM) was evaluated in the NKL [18] and Jurkat cell lines via flow-cytometry. Whereas, IL-2 was a potent stimulus for the generation of p-ERK in the NKL cell line (73.4% of cells positive for p-ERK), this cytokine had virtually no effect on ERK phosphorylation in the Jurkat T cell line at any of the IL-2 doses (4–64 nM) (data not shown). These results were confirmed by immunoblot analysis (Fig. 2 and data not shown). The activation of ERK in response to IL-2 was evaluated in PBMCs isolated from healthy donors ($n = 6$). Cells were treated for 10 min with PBS or different doses of IL-2 and analyzed for p-ERK by intracellular flow-cytometry. Given that, most resting immune cells express the intermediate affinity IL-2R ($K_d = 1$ nM), which is saturated at 10 nM. IL-2, we chose to utilize IL-2 concentrations in the range of 1–128 nM. As with the Jurkat and NKL cell lines, baseline activation of ERK was observed in a small number of PBS-treated cells. The mean percentage

of total PBMCs exhibiting p-ERK in response to IL-2 treatment was significantly higher at the 8 nM dose of IL-2 as compared to untreated cells ($p < 0.0001$) and was significantly greater than the level of activation seen at 4 nM IL-2 concentration ($p = 0.0019$). Furthermore, increasing the doses of IL-2 up to 64 nM did not lead to further significant increase in p-ERK levels (Fig. 3a). Of note, PMA treatments of PBMCs from the same donors routinely lead to the activation of p-ERK in 97% of cells. Results from a representative donor are shown in Fig. 3b. IL-2 induced activation of ERK in PBMCs was modest when measured by immunoblot analysis and it was difficult to distinguish the effects of different IL-2 dosages. However, levels of total ERK were readily detectable in this same population of cells via immunoblot analysis (Fig. 3c). These results indicate that the flow-cytometry technique is highly sensitive and can detect the induction of phosphorylated ERK within a subpopulation of IL-2-activated cells.

p-ERK levels in IL-2-stimulated immune cell subsets

We subsequently developed a dual-parameter flow-cytometric technique to assay the activation of ERK within

Fig. 2 Flow-cytometric analysis of p-ERK in IL-2-stimulated lymphocyte cell lines and validation by immunoblot analysis. NKL and Jurkat T cells were stimulated with PBS or IL-2 (8 nM) for 10 min at 37°C and analyzed for p-ERK by intracellular flow-cytometry. The *x-axis* represents p-ERK, while the *y-axis* represents the forward scatter (FSC) of the gated cells (*upper panel*). Quadrants were set using appropriate isotype control antibodies. The differential expression of the p-ERK protein in these cell lines was confirmed by immunoblot analysis (*lower panel*). Lysates from PBMCs and Jurkat cell lines treated with PMA were used as positive controls for p-ERK expression. Total ERK levels were measured as a loading control



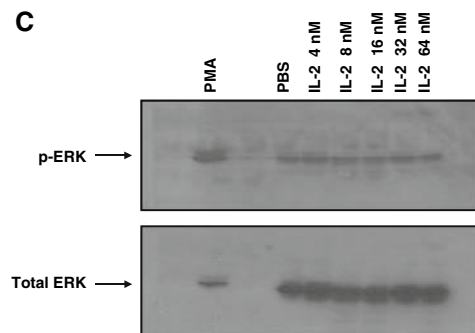
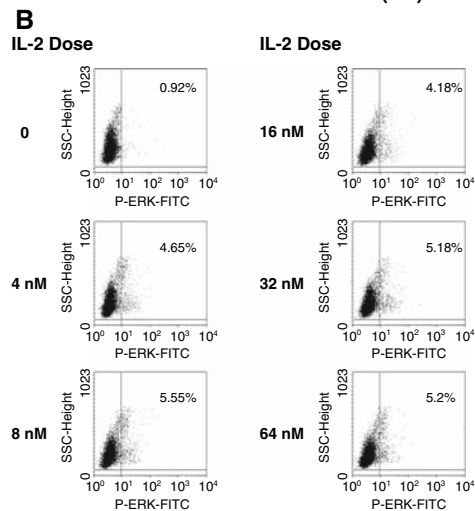
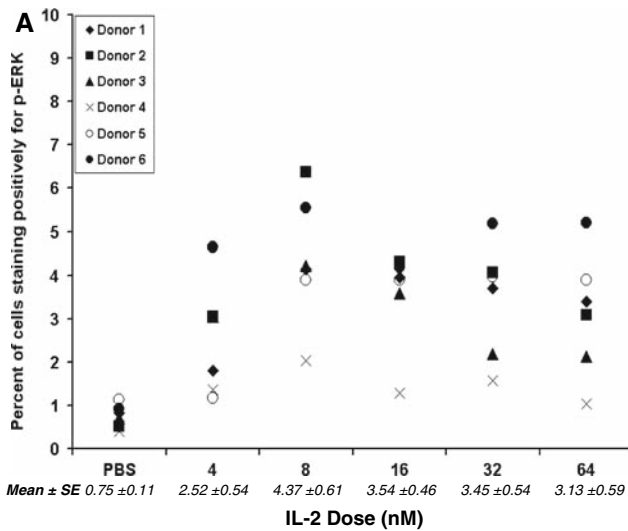
T lymphocytes, NK cells, B cells, and monocytes. Use of this technique revealed that PBMCs treated with IL-2 (8 nM) for 10 min displayed a rapid induction of p-ERK in the NK cell compartment as compared to cells treated with PBS (Fig. 4a). Furthermore, the mean percentage of IL-2 activated cells exhibiting p-ERK was significantly higher in CD56^{bright} NK cells ($65.0 \pm 11.7\%$) as compared to CD56^{dim} NK cells ($10.0 \pm 5.8\%$ for $n = 5$ normal donors, $p < 0.0001$) (Fig. 4b). CD14⁺ monocytes exhibited elevated basal levels of p-ERK ($23.57 \pm 4.87\%$), but there was no significant increase in phosphorylation of ERK following in vitro treatment with IL-2 (4–64 nM) for 10 min ($24.6 \pm 4.9\%$ for $n = 4$ normal donors, $p = 0.219$) (data not shown). However, significant activation of ERK was observed in CD14⁺ monocytes at the 5 min time-point following IL-2 (8 nM) stimulation (Fig. 4a). p-ERK was not observed in CD3⁺ T lymphocytes or in CD21⁺ B cells that had been treated with increasing doses of IL-2 (4–64 nM) over a range of time-points. Dual staining for p-ERK and CD4⁺ or CD8⁺ cells confirmed the lack of ERK activation in the T cell compartment following IL-2 stimulation (data not shown). Of note, PMA-treated PBMCs from the same donors displayed high-levels of p-ERK in every subset tested (Fig. 4a and data not shown).

Time course of ERK activation in IL-2-stimulated immune cell subsets

We further examined the differences in the kinetics of ERK activation following cytokine stimulation within different immune subsets. PBMCs were treated with IL-2 (8 nM) for various periods of time and analyzed for levels of p-ERK within CD56⁺ NK cells and CD14⁺ monocytes, utilizing the dual parameter flow-cytometric technique described above. p-ERK was induced by 5 min in NK cells post IL-2 treatment and peaked at 10 min. Activation of ERK occurred primarily within CD56^{bright} NK cells (Fig. 5a). Additional experiments revealed that the activation of ERK occurred as early as 3 min following IL-2 exposure (data not shown). Phosphorylation of ERK in CD14⁺ monocytes could be detected at 1 min, but peaked around 5 min and then rapidly returned to baseline (Fig. 5b).

ERK activation in CD56^{bright} NK cells

We next isolated pure CD56^{bright} and CD56^{dim} NK cell subsets from three healthy donors via fluorescence-activated cell sorting (FACS) in order to validate the observed difference in ERK activation following IL-2 stimulation. Purified



CD56^{bright} and CD56^{dim} NK cells were treated with IL-2 (8 nM) for 10 min and evaluated for levels of p-ERK by intracellular flow-cytometry. In agreement with our earlier observations, phosphorylation of ERK was much greater in CD56^{bright} NK cells (33.30 ± 12.2%) in response to IL-2 as compared to the CD56^{dim} subset (2.70 ± 1.9%) in three individual donors. Results from a representative donor are shown in Fig. 6. As compared to our earlier studies using freshly isolated PBMCs (Fig. 4b), the levels of IL-2 induced p-ERK in the sorted CD56^{bright} NK cells were

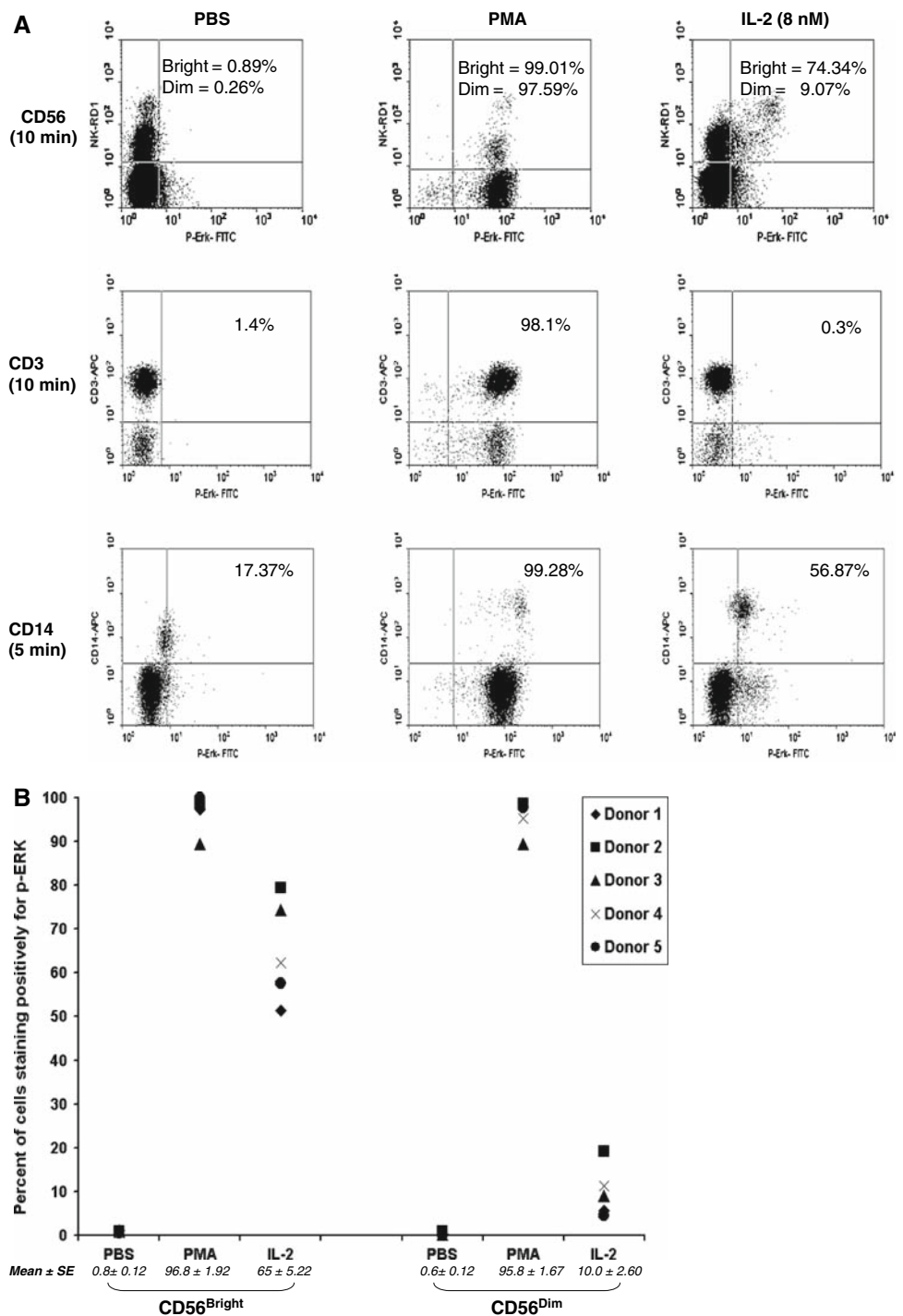
Fig. 3 Flow-cytometric analysis of p-ERK induction in response to IL-2. Freshly isolated PBMCs from healthy donors ($n = 6$) were stimulated with PBS or increasing doses of IL-2 for 10 min at 37°C and evaluated for p-ERK by flow-cytometry. **a** Percent positive cells for p-ERK in total PBMCs obtained from normal donors ($n = 6$) that were stimulated in the presence of IL-2 at the indicated concentrations (4–64 nM). The positive cells for p-ERK were defined as those that displayed fluorescence greater than the background staining obtained with isotype control antibody. The mean p-ERK values obtained from six individual healthy donors and their standard errors (mean ± SE) are shown. **b** Fluorescence data from a single representative individual are presented in a dual parameter plot where the *x-axis* represents p-ERK and the *y-axis* represents the side scatter (SSC) of the lymphocyte- and monocyte-gated cells. Quadrants were set using appropriate isotype control antibodies. **c** An aliquot of cells (5×10^6) was processed to give whole-cell lysates that were subjected to immunoblot analysis with the same anti-p-ERK antibody used for flow-cytometry. PBMCs treated with PMA were used as a positive control. Total ERK levels were measured to confirm equal loading. Representative data are shown

slightly lower. We believe that the manipulation of NK cells during the cell sorting procedure could be the explanation for the modest p-ERK levels in these experiments.

IL-2 receptor expression and p-ERK detection in CD3⁺ T cells

Because CD56^{bright} and CD56^{dim} NK cells exhibited differential phosphorylation of ERK in response to IL-2 treatment, we theorized that the inability of IL-2 to activate ERK in resting CD3⁺ T cells might be due to low-expression of the high-affinity IL-2 receptors (IL-2R $\alpha\beta\gamma$) [16]. Analysis of CD3⁺ T cells from a normal donor revealed that approximately 14.6% of resting CD3⁺ T cells expressed IL-2R α (CD25) and 37.3% of the cells expressed IL-2R γ chain (CD132), whereas the expression of IL-2R β (CD122) was negligible. Following stimulation of T cells via cross-linking of CD3 and CD28, the surface expression of all three IL-2R chains was significantly enhanced (99.9% of activated CD3⁺ T cells expressed CD25, 62.1% expressed CD122, and 83.4% expressed CD132) (Fig. 7a). The effect of IL-2 treatment on the generation of p-ERK in these activated cells was then examined by flow-cytometry. As shown in Fig. 7b, activated CD3⁺ T cells exhibited modest baseline levels of p-ERK as compared to resting cells, presumably due to the activation of ERK via the TCR and CD3 signaling mechanisms [19]. However, the increased expression of the high-affinity IL-2 receptor in the activated CD3⁺ cells did not enhance the activation of ERK in response to IL-2 stimulation. In fact, the levels of p-ERK remained unchanged following IL-2 stimulation in these cells. These findings suggested that the differential response to IL-2 in various immune cellular subsets is not explained by the simple presence or absence of the high-affinity IL-2 receptor.

Fig. 4 Measurement of p-ERK in immune cell subsets by dual parameter flow-cytometry. PBMCs from healthy donors were stimulated with PBS, PMA or IL-2 (8 nM) at 37°C for 10 min and processed for dual parameter flow-cytometry with antibodies to intracellular p-ERK and extracellular surface molecules (CD3, CD14, or CD56). Dual parameter histograms represent cells gated on the lymphocyte population (CD3 or CD56 staining) or the lymphocyte and monocyte populations (CD14 staining). Quadrants were set using appropriate isotype control antibodies for each intra- and extracellular antibody. **a** Staining for p-ERK in immune subsets of PBMCs from a representative donor. **b** p-ERK levels in CD56^{bright} and CD56^{dim} NK cells following stimulation of PBMCs with either PMA or IL-2. Results are shown for ($n = 4$) normal donors. The mean p-ERK values obtained from five individual healthy donors within each subset of CD56⁺ NK cells and their standard errors (mean \pm SE) are shown



Detection of p-ERK in PBMCs from patients undergoing IL-2 immunotherapy

Flow-cytometry was used to analyze ERK phosphorylation in patient immune cells ($n = 8$) obtained immediately prior to, and 1 h following therapy with IL-2 (Table 1). In all patients analyzed, NK cells were noticeably absent in the 1 h post-treatment sample. This occurrence was not surprising and has been documented in a previous report [21].

p-ERK was not evident in either the CD3⁺ or CD21⁺ subset following IL-2 therapy, but p-ERK was observed in the CD14⁺ subset both before and after the administration of IL-2 (Fig. 8 and data not shown). Flow-cytometric analysis also indicated that there was an increase in the total number of circulating CD14⁺ cells in the peripheral blood of all eight patients 1 h following IL-2 administration (mean of CD14⁺ cells = 34.02 \pm 13.7%; 95% CI: 25.58–42.45%; $p < 0.0003$) (See Table 1). In three patients, peripheral

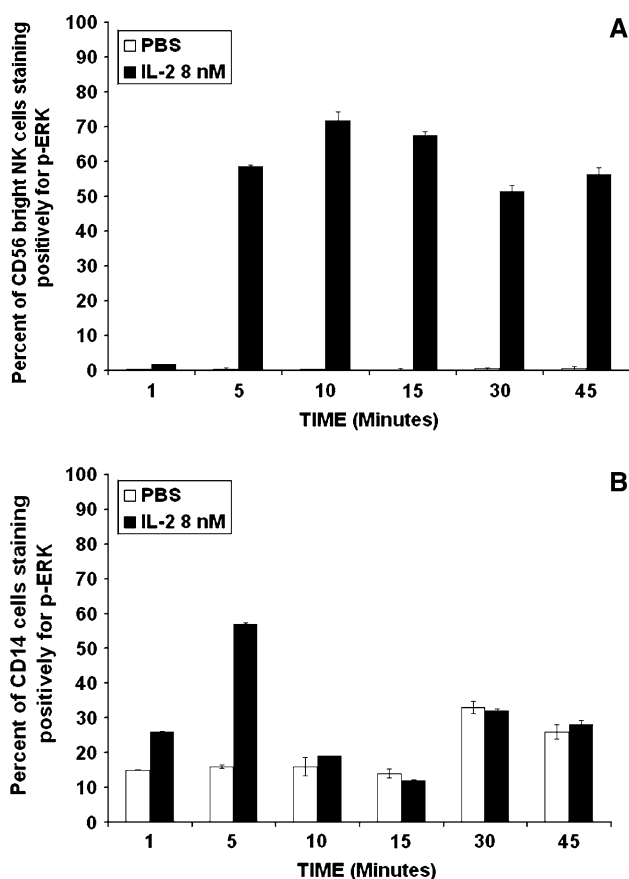
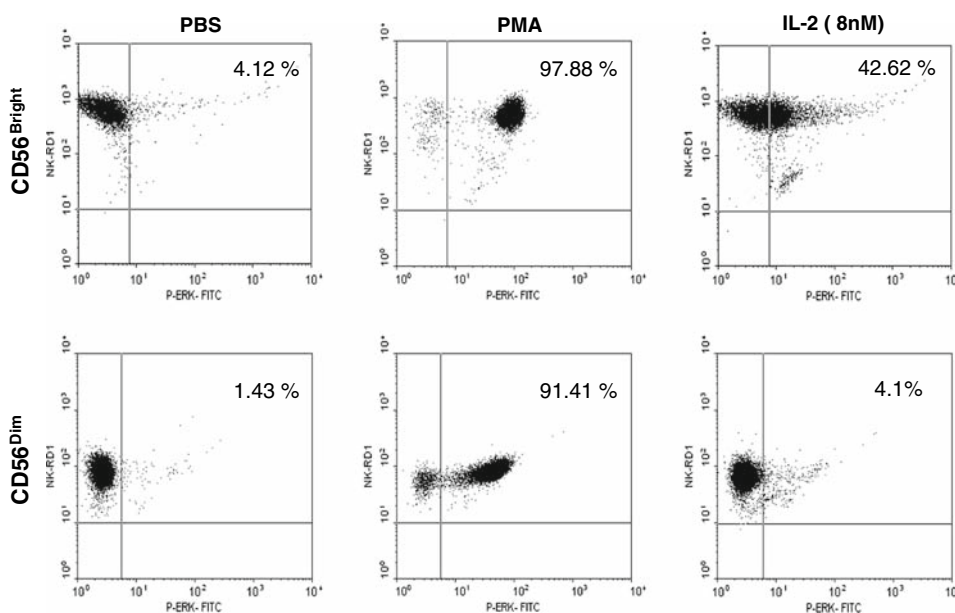


Fig. 5 Time course of p-ERK in IL-2-stimulated immune cell subsets. Freshly isolated PBMCs from healthy donors ($n = 3$) were stimulated with either PBS or IL-2 (8 nM) for increasing lengths of time (1–45 min) and analyzed by dual parameter flow-cytometry for p-ERK in CD3⁺ T cells, CD14⁺ monocytes, and CD56⁺ NK cells. **a** p-ERK levels in IL-2-stimulated CD56^{bright} NK cells for the indicated time. **b** p-ERK levels in IL-2 stimulated CD14⁺ monocytes for the indicated time points. Error bars represent the standard deviation for three data files from each donor

Fig. 6 Validation of ERK activation in CD56^{bright} and CD56^{dim} NK cells. NK cells were isolated from the PBMCs of normal donors ($n = 3$) and further purified for CD56^{bright} and CD56^{dim} NK cell subsets by FACS. Purified cells were stimulated with PBS or IL-2 (8 nM) for 10 min, stained for p-ERK, and analyzed by dual parameter flow-cytometry. p-ERK levels in IL-2-stimulated CD56^{bright} and CD56^{dim} NK cells from a representative donor are shown. The *x*-axis of each histogram represents p-ERK staining, and the *y*-axis represents extracellular NK-RD1 (CD56) staining. Quadrants were set using appropriate isotype control antibodies for intra- and extracellular staining



venous blood was also obtained 3 weeks post-IL-2 treatment and analyzed for p-ERK. Results from a representative patient are shown in Fig. 8 and they reveal persistent activation of ERK in the CD56^{bright} NK cell subset. Interestingly, our group has noted persistent activation of STAT5 in NK cells and T cells at this same time-point. It was also noted that the total number of circulating CD14⁺ monocytes had returned to baseline levels at the 3 week time point post-treatment (6.4% CD14⁺ monocytes at baseline versus 8.5% at 3 weeks post-IL-2 treatment, $n = 3$; $p = 0.9097$).

Discussion

We have developed a dual parametric intracellular flow-cytometric assay to measure IL-2-induced phosphorylation of ERK in immune cells from healthy donors and patients undergoing IL-2 immunotherapy. This method required significantly fewer cells than immunoblot analysis and was highly sensitive. In vitro studies in IL-2-stimulated PBMCs showed that activation of ERK occurred specifically in CD56⁺ NK cells and CD14⁺ monocytes. CD56^{bright} NK cells exhibited a greater degree of ERK phosphorylation than CD56^{dim} NK cells. Phosphorylation of ERK was not seen in naïve CD4⁺, T cells, CD8⁺ T cells, or CD21⁺ B cells upon in vitro stimulation with IL-2. Of note, the induction of high-affinity IL-2 receptors (IL-2R $\alpha\beta\gamma$) on CD3⁺ T cells via treatment with anti-CD3 and anti-CD28 mAbs did not promote the phosphorylation of ERK in response to IL-2. Analysis of patient PBMCs following administration of high-dose IL-2 showed increased levels of activated ERK in monocytes 1 h after treatment. NK cells were absent from blood samples drawn immediately following IL-2

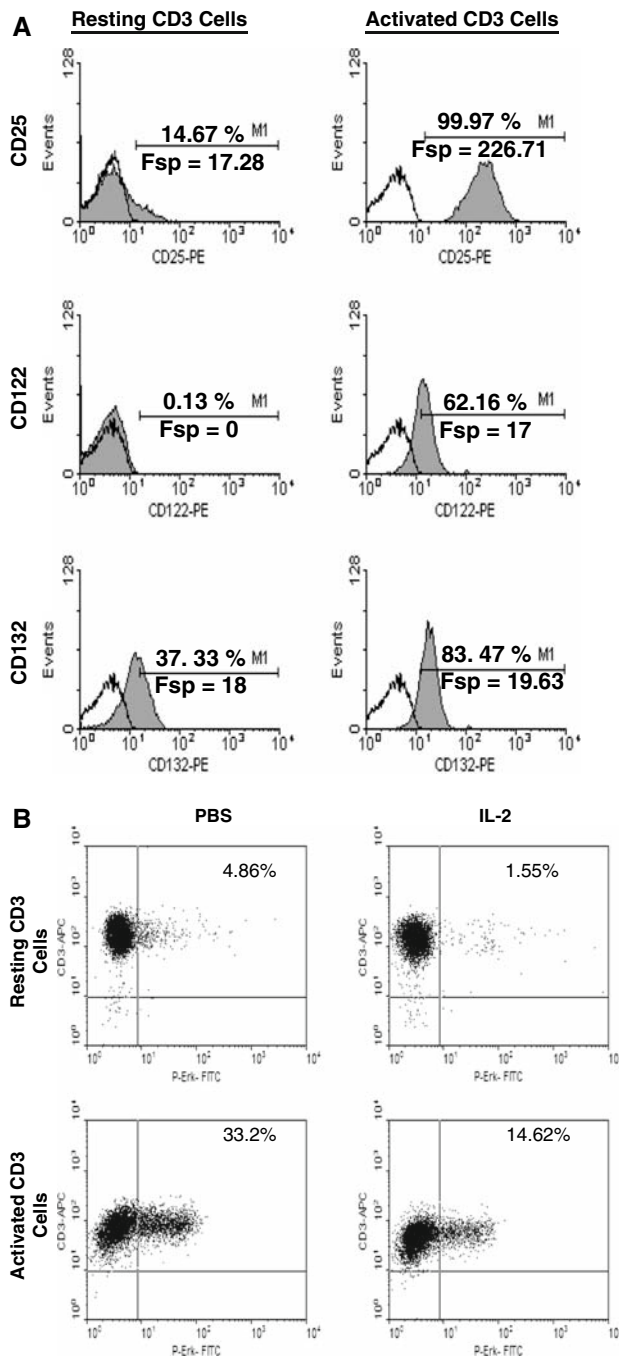


Fig. 7 IL-2R characterization and detection of p-ERK in CD3⁺ T cells. Resting and activated T lymphocytes (CD3⁺ cells) from a normal donor were obtained following a 72 h incubation with CD3/CD28 beads. **a** Cells were stained for surface expression of IL-2R α (CD25), IL-2R β (CD122) or IL-2R γ (CD132) by flow-cytometry. The *solid histograms* represent the specific fluorescence of the indicated receptor subunits (CD25, CD122, or CD132) and the *open histograms* represent the appropriate isotype control antibodies that were used to set markers (M1) in each histogram. Data are presented as the specific fluorescence intensity (Fsp) ($F_{sp} = F_t - F_b$, where F_t = total staining with an anti-CD25, CD122, or CD132 antibody and F_b = total staining with an isotype control antibody and as the percentage of cells positive for CD25, CD122, or CD132 expression (13). **b** Cells were also processed and analyzed for p-ERK levels after stimulation with PBS or IL-2 (64 nM) for 10 min. Dot plots demonstrate p-ERK levels in resting or activated CD3⁺ cells stimulated with PBS or IL-2 (64 nM) for 10 min. The *x-axis* of the histograms represents the p-ERK staining and the *y-axis* represents the extracellular CD3-APC staining. The *upper right quadrant* of the histogram denotes the number of T cells that contained p-ERK

administration, but an analysis of patient blood 3 weeks post-therapy did reveal the presence of p-ERK in the CD56^{bright} NK cells of some patients, possibly due to increased endogenous IL-2. Our findings also suggest that ERK signal transduction in T cells is not a component of the mechanism of action of IL-2 therapy. These results reveal the utility of a flow-cytometric assay for the analysis of activated ERK within immune cell subsets.

This report is the first to evaluate IL-2-induced activation of ERK in immune cell subsets using dual parameter flow-cytometry. Chow et al. [3] utilized single parameter

flow-cytometry to measure activation of ERK following in vitro stimulation of PBMCs with PMA and discovered that the signal strength could be optimized by adjustments in the fixation protocol. PMA was therefore employed as a positive control in the present report, and it routinely induced phosphorylation of ERK in over 97% of immune cells regardless of phenotype. However, we detected IL-2-stimulated ERK phosphorylation only in the CD56⁺ NK cell and CD14⁺ monocyte compartments. Ricciardi et al. employed a flow-cytometric technique to determine that ERK was phosphorylated to a greater extent in G-CSF-mobilized peripheral blood CD34⁺ cells than in normal CD34⁺ bone marrow cells. In this report, markedly elevated levels of p-ERK were observed in over 80% of primary blast cells taken from AML patients, and inhibition of ERK phosphorylation promoted the induction of apoptosis, suggesting a role for this signaling intermediate in maintaining the malignant phenotype [17]. The current method represents a further advance as it permits quantitation of activated ERK within each of the major immune cell subsets following cytokine administration in cancer patients. The high-sensitivity of intracellular flow-cytometry for monitoring cytokine-induced phosphorylation pathways has been confirmed in vitro by other groups using PBMCs [14, 25]. Montag et al. [14] have detected phosphorylated signaling proteins following in vitro treatment of PBMCs with a variety of stimuli (IFN- α , IFN- γ , IL-2, IL-4, IL-10, PMA). The current method represents a further advance as it permits quantitation of activated ERK within each of the major immune cell subsets following in vivo cytokine administration in cancer patients.

NK cells are innate immune effectors that play an important role in host resistance to microbial infections and the elimination of malignant cells. Approximately 90% of NK cells express CD56 at low-density (CD56^{dim}) and cytotoxic in nature by virtue of their expression of the intermediate

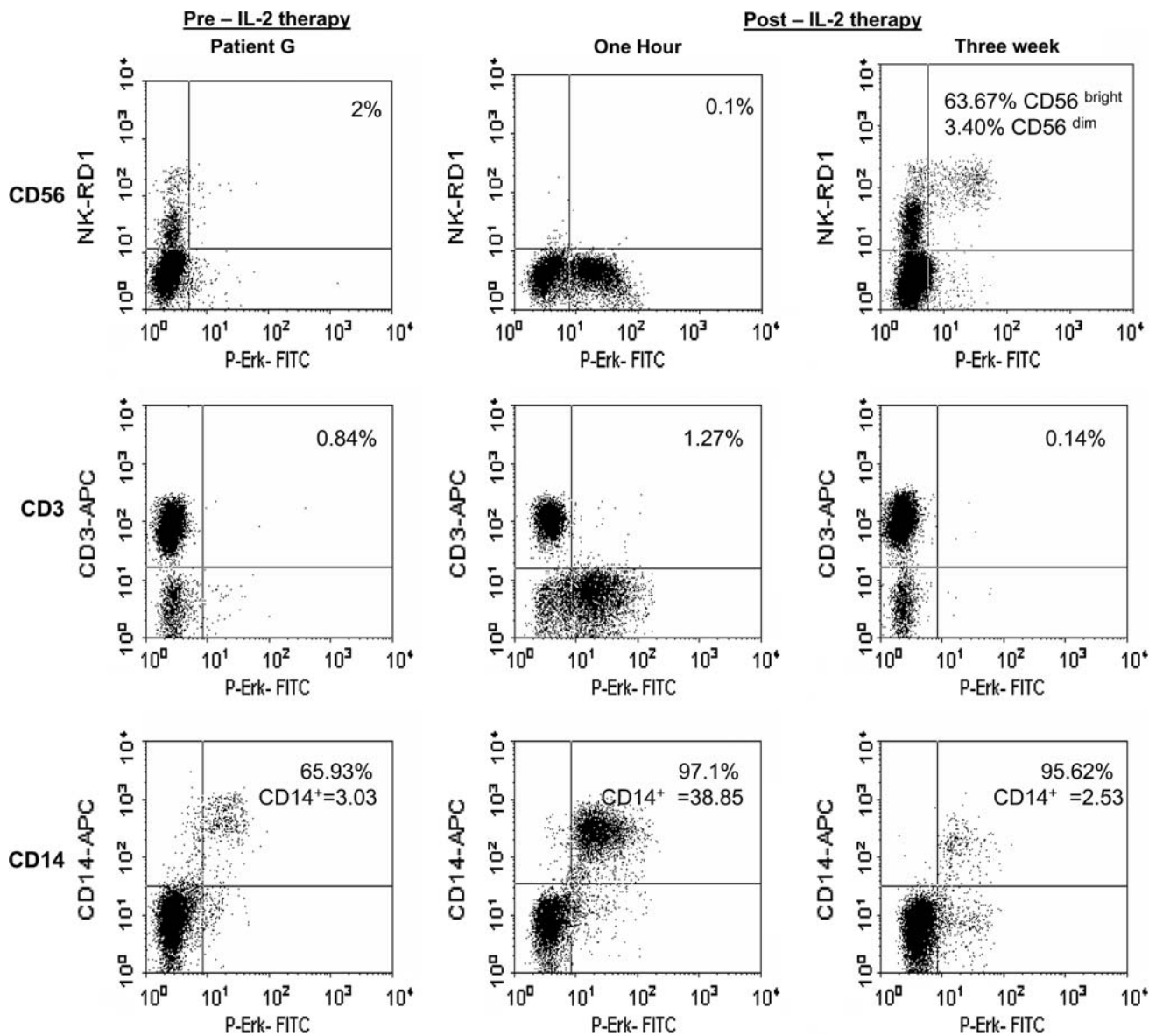


Fig. 8 Detection of p-ERK in lymphocytes from patients undergoing IL-2 immunotherapy. PBMCs were isolated from the peripheral venous blood obtained of patients ($n = 8$) with metastatic melanoma or renal cell carcinoma immediately before, and 1 h and 3 weeks after IL-2 immunotherapy. Cells were analyzed for p-ERK levels within NK cells, T cells, and monocytes by dual parameter flow-cytometry. *Dual parameter histograms* represent cells gated on the lymphocyte popula-

tion (CD3 and CD56 staining) or on the lymphocyte and monocyte populations (CD14 staining). The *x-axis* of each histogram represents p-ERK staining, and the *y-axis* represents extracellular NK-RD1 (NK cells), CD3-APC (T lymphocytes) or CD14-APC (monocytes) staining on four decade logarithmic scales. Representative staining for p-ERK within immune cell subsets in an individual patient prior to, 1 h following, and 3 weeks following in vivo IL-2 immunotherapy is shown

affinity heterodimeric IL-2 receptor (IL-2R $\beta\gamma$). In contrast, CD56^{bright} NK cells are important for their ability to regulate the immune response via cytokine secretion and are characterized by their constitutive expression of the high-affinity heterotrimeric IL-2 receptor (IL-2R $\alpha\beta\gamma$) [5] as well as the heterodimeric receptor. Previous work by Yu et al. [24] using NK cells demonstrated that MAP kinase signaling was required for IL-2-induced generation of LAK cells, IFN- γ secretion and expression of CD25 and CD69. Due to their use of the in vitro kinase reaction to measure ERK phosphor-

ylation, these authors were unable to characterize ERK activation in the two major NK cell subsets. However, our analysis revealed significantly higher levels of p-ERK in CD56^{bright} NK cells ($68.5 \pm 12.23\%$) following in vitro IL-2 stimulation, as compared to the CD56^{dim} NK cells ($13.4 \pm 7.11\%$). Differences between the CD56^{bright} and CD56^{dim} NK cell subsets with respect to ERK phosphorylation suggest that the high-affinity IL-2 receptor of CD56^{bright} NK cells is able to recruit signaling intermediates that are unavailable to cells that express only the heterodimeric form

of the IL-2R. We have also demonstrated that STAT5 was preferentially phosphorylated in CD56^{bright} NK cells obtained from the peripheral blood of some patients with metastatic malignant melanoma who had received high-dose IL-2 1–2 weeks previously [21]. The clinical significance of prolonged IL-2-induced signal transduction in patient NK cells is currently under investigation.

The formation of p-ERK in T cells following IL-2 stimulation remains controversial. Although Ras (upstream of ERK) has been shown to play a role in regulating the growth of IL-2-stimulated T cells [7], it does so in a manner that is independent of Shc and its interactions with the IL-2R β chain [4]. Schade et al. [19] demonstrated that the naïve T cells did not exhibit phosphorylation of ERK following activation with anti-CD3 antibody, while PHA-activated peripheral blood T cells displayed enhanced ERK phosphorylation in response to PHA alone. Interestingly, pre-treatment of PHA-activated T cells with IL-2 potentiated the ability of CD3 antibody treatments to induce the phosphorylation of ERK. Further experiments demonstrated that the enhanced p-ERK response was a result of IL-2-induced activation of the PI-3K pathway. Consistent with these findings, we found that the stimulation of CD3⁺ T cells with anti-CD3 and anti-CD28 Abs (which induced the expression of functional high-affinity IL-2 receptors) led to the generation of p-ERK. However, 15 min exposure of T cells to IL-2 following a 72 h TCR-activation actually diminished the strength of the p-ERK signal. This low-level of ERK phosphorylation in response to IL-2 in T cells expressing the high-affinity IL-2R is in distinct contrast to the strong p-ERK response that was observed in CD56^{bright} NK cells which also bear high-affinity IL-2R. Together, these data suggest that IL-2-induced ERK activation in human T cells is complex, influenced by multiple signaling pathways, and not routinely induced by activation of high-affinity IL-2R.

In summary, we have demonstrated the utility of a dual parametric flow-cytometric assay to detect the activation of ERK in immune effector subsets following IL-2 stimulation. This method may represent a strategy for evaluating the response of individual immune subsets to cytokine therapy at the level of signal transduction.

Acknowledgments This work was supported by National Cancer Institute Grant Numbers P30 CA16058, P01 CA95426, and K24 CA93670, and a grant from Chiron Corporation US-I-IL2-04-028. K.A.V. and D.M.B. are NRSa T32 fellows (5T32 CA09338-27). G.B.L. was supported in part by a research grant from the Melanoma Research Foundation and The Valvano Foundation for Cancer Research. We thank The Ohio State University Comprehensive Cancer Center Analytical Cytometry Shared Resources for help with flow-cytometric studies.

References

- Atkins MB, Kunkel L, Sznol M, Rosenberg SA (2000) High-dose recombinant interleukin-2 therapy in patients with metastatic melanoma: long-term survival update. *Cancer J Sci Am* 6(Suppl 1):S11–S14
- Beadling C, Smith KA (2002) DNA array analysis of interleukin-2-regulated immediate/early genes. *Med Immunol* 1:2
- Chow S, Patel H, Hedley DW (2001) Measurement of MAP kinase activation by flow cytometry using phospho-specific antibodies to MEK and ERK: potential for pharmacodynamic monitoring of signal transduction inhibitors. *Cytometry* 46:72–78
- Evans GA, Goldsmith MA, Johnston JA, Xu W, Weiler SR, Erwin R, Howard OM, Abraham RT, O'Shea JJ, Greene WC et al (1995) Analysis of interleukin-2-dependent signal transduction through the Shc/Grb2 adapter pathway. Interleukin-2-dependent mitogenesis does not require Shc phosphorylation or receptor association. *J Biol Chem* 270:28858–28863
- Farag SS, Caligiuri MA (2006) Human natural killer cell development and biology. *Blood Rev* 20:123–137
- Gesbert F, Delespine-Carmagnat M, Bertoglio J (1998) Recent advances in the understanding of interleukin-2 signal transduction. *J Clin Immunol* 18:307–320
- Graves JD, Downward J, Izquierdo-Pastor M, Rayter S, Warne PH, Cantrell DA (1992) The growth factor IL-2 activates p21ras proteins in normal human T lymphocytes. *J Immunol* 148:2417–2422
- Karin M (1995) The regulation of AP-1 activity by mitogen-activated protein kinases. *J Biol Chem* 270:16483–16486
- Karnitz LM, Abraham RT (1996) Interleukin-2 receptor signaling mechanisms. *Adv Immunol* 61:147–199
- Lesinski GB, Kondadasula SV, Crespin T, Shen L, Kendra K, Walker M, Carson WE 3rd (2004) Multiparametric flow cytometric analysis of inter-patient variation in STAT1 phosphorylation following interferon Alfa immunotherapy. *J Natl Cancer Inst* 96:1331–1342
- Lin JX, Leonard WJ (2000) The role of Stat5a and Stat5b in signaling by IL-2 family cytokines. *Oncogene* 19:2566–2576
- Lissoni P, Bordin V, Vaghi M, Fumagalli L, Bordoni A, Mengo S, Bucovec R, Fumagalli E, Malugani F, Ardizzoia A, Giani L, Gardani GS, Tancini G (2002) Ten-year survival results in metastatic renal cell cancer patients treated with monoimmunotherapy with subcutaneous low-dose interleukin-2. *Anticancer Res* 22:1061–1064
- McDermott DF, Regan MM, Clark JI, Flaherty LE, Weiss GR, Logan TF, Kirkwood JM, Gordon MS, Sosman JA, Ernstoff MS, Tretter CP, Urba WJ, Smith JW, Margolin KA, Mier JW, Gollob JA, Dutcher JP, Atkins MB (2005) Randomized phase III trial of high-dose interleukin-2 versus subcutaneous interleukin-2 and interferon in patients with metastatic renal cell carcinoma. *J Clin Oncol* 23:133–141
- Montag DT, Lotze MT (2006) Successful simultaneous measurement of cell membrane and cytokine induced phosphorylation pathways [CIPP] in human peripheral blood mononuclear cells. *J Immunol Methods* 313:48–60
- Nelson BH (2004) IL-2, regulatory T cells, and tolerance. *J Immunol* 172:3983–3988
- Perola O, Ripatti A, Pelkonen J (2000) T-lymphocyte subpopulations do not express identical combinations of interleukin-2 receptor chains in the early phase of their activation and proliferation. *Scand J Immunol* 52:123–130
- Ricciardi MR, McQueen T, Chism D, Milella M, Estey E, Kaldjian E, Sebolt-Leopold J, Konopleva M, Andreeff M (2005) Quantitative single cell determination of ERK phosphorylation and regulation in relapsed and refractory primary acute myeloid leukemia. *Leukemia* 19:1543–1549
- Robertson MJ, Cochran KJ, Cameron C, Le JM, Tantravahi R, Ritz J (1996) Characterization of a cell line, NKL, derived from an aggressive human natural killer cell leukemia. *Exp Hematol* 24:406–415

19. Schade AE, Levine AD (2004) Cutting edge: extracellular signal-regulated kinases 1/2 function as integrators of TCR signal strength. *J Immunol* 172:5828–5832
20. Theze J, Alzari PM, Bertoglio J (1996) Interleukin 2 and its receptors: recent advances and new immunological functions. *Immunol Today* 17:481–486
21. Varker KA, Kondadasula SV, Go MR, Lesinski GB, Ghosh-Berkebile R, Lehman A, Monk JP, Olencki T, Kendra K, Carson WE 3rd (2006) Multiparametric flow cytometric analysis of signal transducer and activator of transcription 5 phosphorylation in immune cell subsets in vitro and following interleukin-2 immunotherapy. *Clin Cancer Res* 12:5850–5858
22. Wisdom R (1999) AP-1: one switch for many signals. *Exp Cell Res* 253:180–185
23. Yang JC, Sherry RM, Steinberg SM, Topalian SL, Schwartzentruber DJ, Hwu P, Seipp CA, Rogers-Freezer L, Morton KE, White DE, Liewehr DJ, Merino MJ, Rosenberg SA (2003) Randomized study of high-dose and low-dose interleukin-2 in patients with metastatic renal cancer. *J Clin Oncol* 21:3127–3132
24. Yu TK, Caudell EG, Smid C, Grimm EA (2000) IL-2 activation of NK cells: involvement of MKK1/2/ERK but not p38 kinase pathway. *J Immunol* 164:6244–6251
25. Zell T, Khoruts A, Ingulli E, Bonnevier JL, Mueller DL, Jenkins MK (2001) Single-cell analysis of signal transduction in CD4 T cells stimulated by antigen in vivo. *Proc Natl Acad Sci USA* 98:10805–10810